

# Prospects for detection of ultra high frequency gravitational waves from hyperbolic encounters with resonant cavities

Aurélien Barrau,<sup>1,\*</sup> Juan García-Bellido,<sup>2,†</sup> Killian Martineau,<sup>1,‡</sup> and Martin Teuscher<sup>1,3,§</sup>

<sup>1</sup>*Laboratoire de Physique Subatomique et de Cosmologie, Université Grenoble-Alpes, CNRS/IN2P3  
53, avenue des Martyrs, 38026 Grenoble cedex, France*

<sup>2</sup>*Instituto de Física Teórica UAM/CSIC, Universidad Autónoma de Madrid, Cantoblanco 28049 Madrid, Spain*

<sup>3</sup>*École Normale Supérieure de Paris, 45 rue d'Ulm, 75005 Paris, France*

(Dated: April 2024)

In this brief note, we pursue the systematic investigation of possible gravitational wave sources in the gigahertz band. We focus on hyperbolic encounters of light black holes and evaluate precisely the expected signal when accounting for the detailed characteristics of haloscope experiments. Considering the GraHal setup as a benchmark, we insist on the correct signal-to-noise ratio expression taking into account the appropriate timescales. The associated maximum distance – of the order of a few hundreds of astronomical units – at which an event can be detected is calculated for optimal, sub-optimal, and general trajectories.

## I. INTRODUCTION

Observations of gravitational waves (GW) by the LIGO-Virgo collaboration<sup>1</sup> in the  $[10-10^4]$  Hz range have shaken the science of gravity [1]. Since then, the field has blown up, arousing a keen interest that does not cease to grow. At lower frequencies, the LISA project aims at measuring those waves in the  $[10^{-4}-1]$  Hz window [2]. At even lower frequencies, measurements of time delays in pulsar signals by the international pulsar timing array (IPTA) consortium regrouping the North American, European, Indian and Australian Pulsar Timing Arrays (respectively the NANOGrav, EPTA, InPTA and PPTA collaborations) have recently highlighted lines of evidence for a stochastic gravitational wave background in the nHz range [3–5]. Clearly, most of the research effort is dedicated to the exploration of the low frequency region of the spectrum.

The high frequency range, however, remains missing in this landscape. There is a good reason for that: no substantial signal is expected from any known astrophysical source, the upper bound being held by the ringdown signal of neutron star mergers, for which gravitational wave signals of up to 5 kHz are to be expected [6]. On this specific matter of neutron stars physics, some promising counter-arguments were however given in [7].

The absence of known standard sources is obviously not the end of the game as ultra high frequency gravitational wave (UHFGW) signals can be expected from many beyond standard model sources, both in the early or late-time Universe. A review can be found in [8]. Among those potential sources, light primordial black

holes (PBHs) are probably the most natural one [9]. The gravitational signals they can generate, far above the kHz, either through their evaporation or by merging processes, have already been discussed in [9–13]. In this work we focus on another possibility still in the context of primordial black holes: high frequency GW bursts arising from hyperbolic encounters [14–17] in dense clusters of PBHs [18]. Although open trajectories of this kind could be prevalent, they are much less discussed in the literature. We shall show in the following that there are no good reasons for this when both the speed of the frequency drift and the narrow detector bandwidth are taken into account.

When it comes to detection at frequencies above the kHz, various methods have been considered, spanning from optically levitated dielectric sensors operating in the  $[1, 300]$  kHz range [19, 20] to high-energy pulsed lasers at optical frequencies and beyond, up to  $10^{19}$  Hz [21]. These are only examples, and the interested reader can find an exhaustive review in [8]. Among those proposals, resonant cavities located at the core of haloscope experiments (originally designed to search for axionic dark matter), can be reused as competitive GW detectors in the GHz range; see [22] for an introduction and [13] for clarifications regarding the importance of the signal time duration. A novel cavity design specifically dedicated to the search for GWs has also recently been proposed [23].

The goal of this study is to precisely estimate the distance at which a hyperbolic encounter between light black holes can be observed by a resonant cavity operating in the GHz band. We consider the Grenoble Axion Haloscope (GraHal) experiment, described in the third section of the article, as a benchmark. It is currently in the commissioning phase and it should be operational in 2024 [24, 25]

In a nutshell, we find that the distances that could be reached allow to potentially probe events that could

\* [barrau@lpsc.in2p3.fr](mailto:barrau@lpsc.in2p3.fr)

† [juan.garciabellido@gmail.com](mailto:juan.garciabellido@gmail.com)

‡ [martineau@lpsc.in2p3.fr](mailto:martineau@lpsc.in2p3.fr)

§ [martin.teuscher@ens.fr](mailto:martin.teuscher@ens.fr)

<sup>1</sup> Now LIGO-Virgo-Kagra (LVK).

not be noticed otherwise. The smallness of such signals however makes any detection unlikely. Nonetheless, we also find that – maybe surprisingly – the sensitivity is not worse than for bound trajectories. The fundamental reason behind is that, even for inspirals, the time spent within the experimental bandwidth is very small; hence, the hyperbolic case does not drastically differ from the latter. We will carefully consider different kinds of trajectories (from parabolic to highly eccentric) and different mass ratios.

## II. GENERAL CONSIDERATIONS ON HYPERBOLIC ENCOUNTERS

Although highly eccentric trajectories are still to be investigated in details, the case of closed orbits has been intensively considered and the GHz gravitational wave emission is now quite exhaustively understood (see [12, 13]). In principle, hyperbolic encounters should be even more generic – in the sense that unless energy is dissipated it is not possible to gravitationally form a bound system from an unbound one [14–17, 26, 27]. In a recent and more abstract study [28], it was shown that determining the parameters that maximize the strain is not trivial. The most optimal trajectory corresponds to the case where the involved masses are identical, reach the highest possible value allowed by physical constraints and follow a parabola (eccentricity  $e = 1$ ). However, if masses are taken at a given lower value, the most favorable trajectory becomes the one with the *largest* possible eccentricity.

To address the capability of resonant cavities to detect hyperbolic events, the frequency, the strain and the time duration of the phenomenon must be known.

To keep the following analysis as general as possible, we do not specify the individual masses  $m_1$  and  $m_2$  of the black holes and express the results as a function of the reduced mass  $\mu = m_1 m_2 / (m_1 + m_2)$  and the total mass  $M = m_1 + m_2$ . Note that  $\mu$ , and therefore the strain, is maximal when  $m_1 = m_2$  (or  $\mu = M/4$ ).

The characteristic peak frequency of the burst at periapsis can be written in terms of the periapsis radius  $r_p$ , which corresponds to the distance to focus at closest approach, and of the gravitational radius  $R_S = 2GM/c^2$  [28]:

$$f_p = \frac{1}{2\pi} \sqrt{\frac{GM(e+1)}{r_p^3}} \quad (1)$$

$$\approx 1.6 \text{ GHz} \times \left(\frac{10^{-5} M_\odot}{M}\right) \left(\frac{R_S}{r_p}\right)^{\frac{3}{2}} \sqrt{\frac{e+1}{2}},$$

$c$  being the speed of light and  $G$  the gravitational Newton's constant. We shall argue later, in details, why the periapsis region, that corresponds to the maximum strain emission, is the only relevant zone of the path.

Interestingly, the previous expression depends only on the total mass of the system  $M$ , the ratio  $R_S/r_p$ , and the eccentricity  $e$ .

The typical amplitude for the strain is given by [14, 28]:

---


$$\mathfrak{h} \equiv \sqrt{\frac{1}{2} h_{ij}^{\text{TT}} h^{\text{TT} ij}} = \sqrt{h_+^2 + h_\times^2} = \frac{\sqrt{2} G \mu (GM \omega_p)^{2/3}}{D c^4 (e+1)^{4/3}} [8 + 13e^2 + 2e^4 + 2e(12 + 5e^2) \cos \varphi + 13e^2 \cos 2\varphi + 2e^3 \cos 3\varphi]^{1/2}, \quad (2)$$

where  $D$  is the distance to the source and  $\varphi$  the angle along the trajectory. When evaluated at the periapsis, the strain amplitude and the power of the gravitational burst are

$$\mathfrak{h}_{\text{max}} = \mathfrak{h}_p = \frac{2 G \mu (\kappa \omega_p)^{2/3}}{D c^4} \frac{e+2}{(e+1)^{1/3}} \approx 3.6 \times 10^{-25} \times \frac{4q}{(1+q)^2} \frac{G(e)}{G(1)} \left(\frac{M}{10^{-5} M_\odot}\right)^{\frac{5}{3}} \left(\frac{f_p}{1.6 \text{ GHz}}\right)^{\frac{2}{3}} \left(\frac{1 \text{ Mpc}}{D}\right), \quad (3)$$

$$P_{\text{max}} = P_p = \frac{32 G \mu^2 \kappa^4 / 3 \omega_p^{10/3}}{5 c^5 (e+1)^{2/3}} \approx 3.7 \times 10^{24} L_\odot \times \frac{1}{(e+1)^{\frac{2}{3}}} \left(\frac{4q}{(1+q)^2}\right)^2 \left(\frac{M}{10^{-5} M_\odot}\right)^{\frac{10}{3}} \left(\frac{f_p}{1.6 \text{ GHz}}\right)^{\frac{10}{3}}, \quad (4)$$

where  $L_\odot$  is the solar luminosity. In the above the following functions  $G(e) \equiv e + 2/(e+1)^{1/3}$ ,  $H(e) \equiv e + 2/(e+1)^2$  and the ratio  $q \equiv m_1/m_2$  have been introduced.

From now on, the pulsation  $\omega_p$  of the generated burst

---

at the periapsis is set equal to the detector frequency  $\nu$ , such that  $\omega_p = 2\pi\nu$ .

The time duration of the signal in a detector bandwidth  $\Delta\nu$  centered around an operating frequency  $\nu$  can be computed using the conservation of momentum

[14, 28]:

$$t_{\Delta\nu}(\nu, \Delta\nu, e) = \frac{1}{\pi\nu} \sqrt{1 + \frac{1}{e}} \sqrt{\frac{\Delta\nu}{\nu}}. \quad (5)$$

Since  $\nu$  and  $\Delta\nu$  are fixed by the experimental apparatus, this time duration depends only on the eccentricity  $e \geq 1$  of the hyperbolic trajectory.

### III. EXPERIMENTAL SETUP

One of the most promising possibilities to search for GWs around the GHz is to re-use resonant cavities located inside haloscope instruments, originally dedicated to axion-like particle searches [8, 22]. For signals that would remain coherent for very long times, already existing experiments exhibit impressive sensitivities on the strain, reaching  $h \sim 10^{-22}$  [22]. It was however emphasized in [12, 13] that the time  $t_{\Delta\nu}$  spent by the signal within the sensitivity band of the detector is crucial when estimating the signal to noise ratio (SNR). In principle, maximizing the strain is not necessarily equivalent to maximizing the SNR. For haloscope experiments, the usual Dicke radiometer formula [22, 29, 30] reads

$$\text{SNR} \sim \frac{P_{\text{sig}}}{k_B T_{\text{sys}}} \sqrt{\frac{t_{\text{eff}}}{\Delta\nu}}, \quad (6)$$

$P_{\text{sig}}$  being the signal power,  $k_B$  the Boltzmann constant,  $T_{\text{sys}}$  the temperature of the system (that includes all contributions),  $\Delta\nu$  the spectral bandwidth, and  $t_{\text{eff}}$  the effective time during which the detector gathers enough signal. The expression of this effective time is discussed in detail below.

The power associated with GW signals has been estimated to be [22]:

$$P_{\text{sig}} = \frac{1}{2\mu_0 c^2} V_{\text{cav}}^{5/3} (\eta B_0)^2 Q (2\pi\nu)^3 h^2, \quad (7)$$

in which  $\mu_0$  is the vacuum magnetic permeability and  $V_{\text{cav}}$ ,  $\eta$ ,  $B_0$ ,  $Q$  are respectively the volume of the cavity, the coupling coefficient between gravitational waves and resonance modes, the static magnetic field inside the cavity, and the quality factor.

This raises an important point: *the quantity to maximize, at a fixed given frequency, in order to reach the best sensitivity is  $h^2 \sqrt{t_{\text{eff}}}$  rather than  $h$  itself.* We have however shown in [28] that, in practice, for hyperbolic trajectories, the highest signal (in the sense of  $h^2 \sqrt{t_{\text{eff}}}$ ) is always reached at the periapsis.

Numerical estimates of the observational distance require the experimental quantities of interest to be specified. To do so, we use the GrAHal experiment as a benchmark. Initially designed for the search of axionic dark matter in our galactic halo, GrAHal is a haloscope

platform located in Grenoble [31, 32] whose development has been motivated by the existence on site of a 43 Tesla multiconfiguration hybrid magnet. Table I presents the parameters relevant for this study, for five different configurations accessible at the GrAHal platform. Introducing  $T_{\text{cav}}$  as the cavity temperature, the benchmark for the system temperature appearing in this table corresponds to the sum of three terms: the amplifier noise temperature, which dominates, the cavity thermal noise  $h\nu / (\exp[h\nu / k_B T_{\text{cav}}] - 1)$ , and the zero-point fluctuations of the blackbody gas. The frequency of the transverse-magnetic mode  $\nu_{TM010}$  provided in this table will, from now on, be considered as the operating frequency of the detector  $\nu = \omega_p / 2\pi = \nu_{TM010}$ .

GrAHal configurations			
$B_0$ (T)	Cavity volume ( $\text{m}^3$ )	$T_{\text{sys}}$ (K)	$\nu_{TM010}$ (GHz)
9	$5.01 \times 10^{-1}$	0.3	0.34
17.5	$3.22 \times 10^{-2}$	0.3	0.79
27	$1.83 \times 10^{-3}$	0.4	2.67
40	$1.42 \times 10^{-4}$	1.0	6.74
43	$4.93 \times 10^{-5}$	1.0	11.47

TABLE I. Main possible configurations for GrAHal using the 43 T Grenoble hybrid magnet [24, 25].

To perform sensitivity estimates, the effective time  $t_{\text{eff}}$  appearing in the signal-to-noise ratio has to be specified. It depends on the time  $t_{\Delta\nu}$  during which the evolving gravitational wave frequency drifts into the sensitivity bandwidth of the experiment  $\Delta\nu$ , but also on timescales relevant for the experiment, such as the maximal integration time  $t_{\text{max}}$  or the inverse sampling rate  $t_{\text{min}} = 1/\Delta\nu$ .

We have shown in [13] that three regimes should *a priori* be distinguished depending on the hierarchy between  $t_{\text{min}}$ ,  $t_{\text{max}}$ , and  $t_{\Delta\nu}$ . It is however easy to show that the condition  $t_{\Delta\nu} < t_{\text{min}}$  is equivalent to  $Q^{-3/2} < 1$  for hyperbolic trajectories, which is obviously satisfied. The case in which the signal duration in the detector bandwidth is smaller than the time separating two successive samples is therefore the only regime which needs to be considered in this work and the corresponding loss in SNR is taken into account by setting  $t_{\text{eff}} = t_{\Delta\nu}^2 / t_{\text{min}}$  [13].

Numerical estimates are obtained using Eq. (5) in the specific case of a resonant cavity. This leads to

$$t_{\Delta\nu} \approx 10^{-13} \text{ s} \times \left( \frac{2.67 \text{ GHz}}{\nu} \right) \left( \frac{10^5}{Q} \right)^{1/2}. \quad (8)$$

### IV. MAXIMAL DISTANCE ACCESSIBLE

The estimation of the maximum accessible distance, basically obtained by requiring  $\text{SNR} > 5$ , depends both on the sensitivity of the experiment on the strain and

duration of the emitted signal.

### A. General considerations and strain sensitivity

Before performing the detailed estimates, it is worth underlying an important point to emphasize more clearly why we focus on the periapsis throughout all this study.

In [13], it has been shown that, in the case of a coalescing system, the sensitivity on the strain is maximal for the *lowest* black hole masses and decreases as the chirp mass of the system increases. This simply reflects the fact that the lower the mass, the earlier the binary system is considered in its inspiral phase, and the longer the signal remains inside the detector bandwidth. Focusing on the dynamics long before the merging, it is always possible to find parameters such that the signal spends an arbitrary large amount of time within the experiment bandwidth. In this case, the required strain to get a measurable signal obviously gets smaller.

Of course, this does not mean that lower masses are more likely to be observed as the emitted signal decreases when the chirp mass decreases. The increase in  $t_{\Delta\nu}$  never comes close to compensate for the decrease in strain (see figures 4 and 5 of [13]).

---


$$\begin{aligned} h_{\min} &= \sqrt{\frac{\mu_0 c^2 k B}{4\pi^2}} \text{SNR}^{\frac{1}{2}} T_{\text{sys}}^{\frac{1}{2}} V_{\text{cav}}^{-\frac{5}{6}} \eta^{-1} B_0^{-1} \nu^{-1} Q^{\frac{1}{4}} \left(1 + \frac{1}{e}\right)^{-\frac{1}{4}} \\ &\simeq 1.6 \times 10^{-13} \left(\frac{\text{SNR}}{5}\right)^{\frac{1}{2}} \left(\frac{T_{\text{sys}}}{0.4 \text{ K}}\right)^{\frac{1}{2}} \left(\frac{1.83 \times 10^{-3} \text{ m}^3}{V_{\text{cav}}}\right)^{\frac{5}{6}} \left(\frac{0.1}{\eta}\right) \left(\frac{27 \text{ T}}{B_0}\right) \left(\frac{2.67 \text{ GHz}}{\nu}\right) \left(\frac{Q}{10^5}\right)^{\frac{1}{4}} \left(\frac{2e}{1+e}\right)^{\frac{1}{4}}. \end{aligned} \quad (9)$$

It is important to notice that, for standard fiducial parameters, the numerical value obtained here is far above the sensitivity around  $10^{-22}$  for long time coherent signals [22]. The reason for this apparent loss in sensitivity is obviously not the experiment itself, but the extremely small time duration of the signal, as reflected by Eq. (8). As discussed previously, considering parts of the hyperbolic trajectory which increase  $t_{\Delta\nu}$  would decrease the required strain for detection but would still dramatically worsen the distance at which an event could be seen. The value of  $h_{\min}$  calculated in this work is consistent with the results we have previously obtained for coalescing systems [13]. Should the orbit be elliptic or hyperbolic, the time spent by the signal in the (very high frequency) detector bandwidth would be roughly the same (as it is anyway smaller than the orbital period) as soon as one focuses on the most favourable case, that is the largest masses.

In the case of hyperbolic encounters, the same argument could, in principle, be made. The instantaneous (mean) value of the frequency of the signal does indeed decrease continuously when the system is considered far away from the periapsis. In this case, speeds are smaller, hence the system stays longer in the bandwidth. The frequency at the periapsis should then be much above the experiment frequency. However, in addition to the already drastic decrease in SNR described in [13] and mainly due to the necessarily smaller masses involved in the process, two additional effects make this situation even more marginal for open trajectories than for bounded ones. First, as soon as the trajectory is considered far away from the periapsis, the Fourier transform of the signal gets wider and the amount of signal within the bandwidth of the experiment decreases. Second, the trajectory becomes nearly linear and, therefore, even at fixed masses, the signal would be strongly damped.

For all those reasons, we consider only the signal emitted around the periapsis. As the system basically stays here for half a period, it is impossible that it spends a vast amount of time within the bandwidth while emitting UHFGWs.

Plugging Eqs. (5) and (7) into Eq. (6) it is straightforward to estimate the minimum strain that can be detected:

---

### B. Description of the parameter space

The typical strain  $h$ , normalized at a distance of 1 Mpc, is plotted as a function of eccentricity and total mass in Fig. 1, assuming  $m_1 = m_2$  and a periapsis frequencies given by typical values of the  $\nu_{TM010}$  mode of GrAHal. As this work is specifically focused on signals in resonant cavities and not on the mathematical aspects of GW emission along the trajectory, we refer the interested reader to [28] to get details about the ingredients necessary for this plot.

We impose two different constrains on the system:

- the relative velocity between the two masses should not exceed the speed of light, *i.e.*  $v_{\max} < c$ ;
- the system should not merge, *i.e.*  $r_{\min} > R_S$ .

Under those constrains, all eccentricities are bounded by

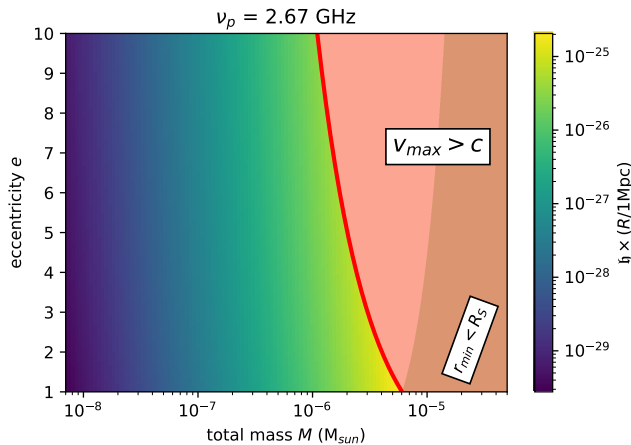


FIG. 1. Emitted strain  $\mathfrak{h}$  as a function of eccentricity and total mass of the system, for a frequency at periapsis  $\omega_p/(2\pi)$  fixed at the detector frequency  $\nu = 2.67$  GHz and considering  $m_1 = m_2$ . The solid red line  $e = e_*(M, \omega_p)$  is the dividing line between physically allowed and excluded regions of the parameter space, considering two constrains: the “no-merging” constrain  $r_{\min} > R_S$  and the “maximal allowed speed” constrain  $v_{\max} < c$ . As demonstrated in section III B of [28], the intersection between this dividing line and the  $e = 1$  line is the point of the parameter space where  $\mathfrak{h}$  is maximal. When one variable is fixed, the strain evolves as  $\mathfrak{h} \propto M^{5/3}$  or  $\mathfrak{h} \propto e^{2/3}$  (for sufficiently large values of  $e$ ).

$$e \leq e_* = \frac{c^3}{GM\omega_p} - 1. \quad (10)$$

The accessible masses are therefore given by:

$$M \leq 6.1 \times 10^{-6} M_\odot \left( \frac{2}{e+1} \right) \left( \frac{2\pi \times 2.67 \text{ GHz}}{\omega_p} \right), \quad (11)$$

the highest value corresponding to the parabolic trajectory  $e = 1$ .

We now consider three different relevant situations:

- The so-called “general case”, filling almost all the allowed region of the parameter space;
- The “optimized trajectories”, that correspond to trajectories that maximize the strain at fixed  $e$  or  $M$ . These are the trajectories that lie along the curve corresponding to the constraint  $e = e_*$ ;
- The “parabolic trajectory” given by  $e_* = 1$ . Even though being a single point in the previous parameter space, we still discuss it as it is trajectory that saturates the constraint  $e = e_*$  while corresponding to the highest  $M$  accessible. As a result, this trajectory is the one generating the highest strain.

### C. General case

Using the previous formulas for the strain and time duration of the signal, given by Eqs. (3) and (5), in the expression of the SNR (6), one is led to a maximal distance for a detectable event given by:

$$\begin{aligned} D_{\max} &= \frac{2^{2/3} \pi^{5/3}}{\sqrt{\text{SNR}}} \frac{G^{5/3}}{c^5 \sqrt{\mu_0 k_B}} \frac{V_{\text{cav}}^{5/6} \eta B_0 \nu^{5/3} Q^{1/4}}{\sqrt{T_{\text{sys}}}} \quad (12) \\ &\times \frac{4\mu}{M} M^{5/3} G(e) \\ &= \frac{6.1 \text{ AU}}{\sqrt{\text{SNR}}} \left( \frac{V_{\text{cav}}}{1.83 \times 10^{-3} \text{ m}^3} \right)^{5/6} \left( \frac{\eta}{0.1} \right) \left( \frac{B_0}{27 \text{ T}} \right) \times \\ &\left( \frac{\nu}{2.67 \text{ GHz}} \right)^{5/3} \left( \frac{Q}{10^5} \right)^{1/4} \left( \frac{T_{\text{sys}}}{0.4 \text{ K}} \right)^{-1/2} \times \\ &\left( \frac{G(e)}{G(1)} \right) \left( \frac{M}{6.1 \times 10^{-8} M_\odot} \right)^{5/3} \left( \frac{4\mu}{M} \right), \quad (13) \end{aligned}$$

where “AU” stands for astronomical unit and

$$G(e) \equiv \frac{e+2}{(e+1)^{1/3}} \left( 1 + \frac{1}{e} \right)^{1/4}. \quad (14)$$

For all  $e \geq 1$ ,  $G(e)$  is a monotonously increasing function of  $e$  that takes values  $G(1) \simeq 2.8$  and  $G(10) \simeq 5.5$ . The  $4\mu/M$  factor becomes one when the two black hole masses are the same (this situation also corresponds to the one that maximizes the emitted strain  $\mathfrak{h}$ ).

### D. Optimized trajectories

In this section, we focus on favourable situations.

As demonstrated in [28], and somehow counter intuitively, at fixed total mass  $M$ , the trajectory that maximizes the SNR keeping the constraint that the periapsis frequency is fixed at the detector frequency (as in the III. B. case of [28]), is the one with the *highest* eccentricity.

Those trajectories are such that the black hole masses and the periapsis frequency are not independent variables. If the gravitational wave frequency at the periapsis is taken to be the one of the detector, this fixes the total mass of the observed system such that:

$$\begin{aligned} M &= \frac{c^3}{(e+1)2\pi G\nu_p} \quad (15) \\ &= 1.1 \times 10^{-5} M_\odot \left( \frac{1}{e+1} \right) \left( \frac{2.87 \text{ GHz}}{\nu} \right). \quad (16) \end{aligned}$$

The maximal distance at which an event is accessible becomes

$$D_{\max} = \frac{1}{2\sqrt{\text{SNR}}} \frac{V_{\text{cav}}^{5/6} \eta B_0}{\sqrt{\mu_0 k_B T_{\text{sys}}}} \frac{4\mu}{M} Q^{1/4} H(e) \quad (17)$$

$$= \frac{253 \text{ AU}}{\sqrt{\text{SNR}}} \left( \frac{4\mu}{M} \right) \left( \frac{V_{\text{cav}}}{1.83 \times 10^{-3} \text{ m}^3} \right)^{5/6} \left( \frac{\eta}{0.1} \right) \times \left( \frac{B_0}{27 \text{ T}} \right) \left( \frac{T_{\text{sys}}}{0.4 \text{ K}} \right)^{-1/2} \left( \frac{Q}{10^5} \right)^{1/4} \times H(e), \quad (18)$$

$$\text{with } H(e) \equiv \frac{e+2}{e^{1/4}(e+1)^{7/4}}.$$

Let us now focus on the “most optimal” trajectory, which corresponds to the case where the involved masses (assumed here to be the same) reach the higher possible value allowed by physical constraints and follow a parabola (eccentricity  $e = 1$ ). The parabolic limit of Eq. (5) is:

$$t_{\Delta\nu} = \frac{\sqrt{2}}{\pi\nu} \sqrt{\frac{\Delta\nu}{\nu}} \quad (19)$$

$$= 5.3 \times 10^{-13} \text{ s} \times \frac{2.67 \times 10^9 \text{ Hz}}{\nu} \left( \frac{10^5}{Q} \right)^{1/2} \quad (20)$$

Then, using (15) and previous equations for  $e = 1$ :

$$D_{\max} = \frac{3}{2^{11/4} \sqrt{\text{SNR}}} \frac{V_{\text{cav}}^{5/6} \eta B_0}{\sqrt{\mu_0 k_B T_{\text{sys}}}} \frac{4\mu}{M} Q^{1/4} \quad (21)$$

$$= \frac{284 \text{ AU}}{\sqrt{\text{SNR}}} \left( \frac{V_{\text{cav}}}{4.93 \times 10^{-5} \text{ m}^3} \right)^{5/6} \times \left( \frac{\eta}{0.1} \right) \left( \frac{B_0}{43 \text{ T}} \right) \left( \frac{T_{\text{sys}}}{1.0 \text{ K}} \right)^{-1/2} \left( \frac{Q}{10^5} \right)^{1/4}. \quad (22)$$

### E. Discussion

For fiducial parameters close to those expected for the GrAHal experiment, the maximum distance at which an event could be detected is of the order of a few hundreds? of astronomical units in the best case. This is significant in the sense that a pair of  $10^{-6} M_{\odot}$  black holes at this distance would have gone otherwise unnoticed. If one remains agnostic about the actual cause of the event, it is indeed worth considering this type of encounters. It does not conflict with any known observation and could be detected by resonant cavities. This might even be the only way to probe such phenomena. It is quite impressive that two black holes of millimeter size could,

in principle, be detected much farther away than the Sun.

On the other hand, if one assumes that dark matter is made of such black holes and estimates the event rate following the approach of [14], the result is extraordinary low. Whatever the reasonable values of the parameters one is led to much less than one event per Hubble time. It would therefore require a very exotic scenario for events of this kind to happen during the lifetime of the experiment. This is the main conclusion of this work.

## V. CONCLUSION

In this brief article, we have investigated the detection capability of resonant cavities operating in the GHz range for hyperbolic encounters of light black holes. It might have been expected that the maximum distance at which an event can be detected is much less than in the case of a bound orbit for which the signal is assumed to be integrated over many cycles. In a hyperbolic encounter, the considered frequency (and amplitude) is attained only during a fraction (typically one half) of the associated orbital period. The naive reasoning is however misleading as, even for a closed orbit, the frequency drift is so fast – for the highest masses accessible, which are the most relevant ones – that it is anyway measured during a timescale smaller than an orbital period. This is why the distances found in this work are of the same order of magnitude than those previously estimated for coalescing systems. Slight differences come from considering black holes grazing each other (in the hyperbolic case) instead of being at the ISCO (in the circular case).

In principle, the calculated distances, of the order of a few hundreds of astronomical units, are relevant in the sense that an encounter taking place this far away would not be detectable by any other means. Its occurrence possibility is not ruled out by any existing observation and involves black hole masses that are compatible with inflationary scenarios known to produce PBHs.

However, the distances remain extremely small at the cosmological – or even galactic – scale and the expected event rate would be ridiculously tiny for any smooth distribution of dark matter black holes. This makes the possibility of using GHz resonant cavities as a probe of light black holes very unlikely.

In a future work, beyond the scope of this note, it could be welcome to refine the estimation of the event rate and widen the analysis to lower frequencies.

[1] R. Abbott *et al.* (KAGRA, VIRGO, LIGO Scientific), *Phys. Rev. X* **13**, 041039 (2023), arXiv:2111.03606 [gr-

qc].

[2] L. collaboration, “Laser interferometer space antenna,”

- (2017), [arXiv:1702.00786 \[astro-ph.IM\]](#).
- [3] G. Agazie *et al.* (NANOGrav), *Astrophys. J. Lett.* **951**, L8 (2023), [arXiv:2306.16213 \[astro-ph.HE\]](#).
- [4] J. Antoniadis *et al.* (EPTA, InPTA:), *Astron. Astrophys.* **678**, A50 (2023), [arXiv:2306.16214 \[astro-ph.HE\]](#).
- [5] D. J. Reardon *et al.*, *Astrophys. J. Lett.* **951**, L6 (2023), [arXiv:2306.16215 \[astro-ph.HE\]](#).
- [6] A. Bauswein, N. Stergioulas, and H.-T. Janka, *Eur. Phys. J. A* **52**, 56 (2016), [arXiv:1508.05493 \[astro-ph.HE\]](#).
- [7] J. Casalderrey-Solana, D. Mateos, and M. Sanchez-Garitaonandia, “Mega-hertz gravitational waves from neutron star mergers,” (2022), [arXiv:2210.03171 \[hep-th\]](#).
- [8] N. Aggarwal *et al.*, *Living Rev. Rel.* **24**, 4 (2021), [arXiv:2011.12414 \[gr-qc\]](#).
- [9] E. Bagui *et al.* (LISA Cosmology Working Group), “Primordial black holes and their gravitational-wave signatures,” (2023), [arXiv:2310.19857 \[astro-ph.CO\]](#).
- [10] R. Anantua, R. Easther, and J. T. Giblin, *Phys. Rev. Lett.* **103**, 111303 (2009), [arXiv:0812.0825 \[astro-ph\]](#).
- [11] R. Dong, W. H. Kinney, and D. Stojkovic, *JCAP*, 034 (2016), [arXiv:1511.05642 \[astro-ph.CO\]](#).
- [12] G. Franciolini, A. Maharana, and F. Muia, *Phys. Rev. D* **106**, 103520 (2022), [arXiv:2205.02153 \[astro-ph.CO\]](#).
- [13] A. Barrau, J. García-Bellido, T. Grenet, and K. Martineau, “Prospects for detection of ultra high frequency gravitational waves from compact binary coalescences with resonant cavities,” (2023), [arXiv:2303.06006 \[gr-qc\]](#).
- [14] J. García-Bellido and S. Nesseris, *Phys. Dark Univ.* **21**, 61 (2018), [arXiv:1711.09702 \[astro-ph.HE\]](#).
- [15] J. García-Bellido and S. Nesseris, *Phys. Dark Univ.* **18**, 123 (2017), [arXiv:1706.02111 \[astro-ph.CO\]](#).
- [16] G. Morrás, J. García-Bellido, and S. Nesseris, *Phys. Dark Univ.* **35**, 100932 (2022), [arXiv:2110.08000 \[astro-ph.HE\]](#).
- [17] J. García-Bellido, S. Jaraba, and S. Kuroyanagi, *Phys. Dark Univ.* **36**, 101009 (2022), [arXiv:2109.11376 \[gr-qc\]](#).
- [18] M. Trashorras, J. García-Bellido, and S. Nesseris, *Universe* **7**, 18 (2021), [arXiv:2006.15018 \[astro-ph.CO\]](#).
- [19] A. Arvanitaki and A. A. Geraci, *Phys. Rev. Lett.* **110**, 071105 (2013), [arXiv:1207.5320 \[gr-qc\]](#).
- [20] N. Aggarwal, G. P. Winstone, M. Teo, M. Baryakhtar, S. L. Larson, V. Kalogera, and A. A. Geraci, *Phys. Rev. Lett.* **128**, 111101 (2022), [arXiv:2010.13157 \[gr-qc\]](#).
- [21] G. Vacalis, G. Marocco, J. Bamber, R. Bingham, and G. Gregori, *Class. Quant. Grav.* **40**, 155006 (2023), [arXiv:2301.08163 \[gr-qc\]](#).
- [22] A. Berlin, D. Blas, R. Tito D’Agnolo, S. A. R. Ellis, R. Harnik, Y. Kahn, and J. Schütte-Engel, *Phys. Rev. D* **105**, 116011 (2022), [arXiv:2112.11465 \[hep-ph\]](#).
- [23] P. Navarro, B. Gimeno, J. Monzón-Cabrera, A. Díaz-Morcillo, and D. Blas, “Study of a cubic cavity resonator for gravitational waves detection in the microwave frequency range,” (2023), [arXiv:2312.02270 \[hep-ph\]](#).
- [24] P. Pugnât, R. Barbier, C. Berriaud, R. Berthier, T. Boujet, P. Graffin, C. Grandclément, B. Hervieu, J. Jousset, F. P. Juster, M. Kamke, F. Molinié, H. Neyrial, M. Pelloux, R. Pfister, L. Ronayette, H. J. Schneider-Muntau, E. Verney, and E. Yildiz, *IEEE Transactions on Applied Superconductivity* **32**, 1 (2022).
- [25] P. Pugnât, R. Barbier, C. Berriaud, F. Debray, C. Grandclément, B. Hervieu, S. Kramer, Y. Krupko, F. Molinié, M. Pelloux, R. Pfister, L. Ronayette, and H. J. Schneider-Muntau, *IEEE Transactions on Applied Superconductivity* **34**, 1 (2024).
- [26] S. Jaraba and J. Garcia-Bellido, *Phys. Dark Univ.* **34**, 100882 (2021), [arXiv:2106.01436 \[gr-qc\]](#).
- [27] M. Caldarola, S. Kuroyanagi, S. Nesseris, and J. Garcia-Bellido, “The effects of orbital precession on hyperbolic encounters,” (2023), [arXiv:2307.00915 \[gr-qc\]](#).
- [28] M. Teuscher, A. Barrau, and K. Martineau, “Elementary considerations on gravitational waves from hyperbolic encounters,” (2024), [arXiv:2402.10706 \[gr-qc\]](#).
- [29] P. Sikivie, *Rev. Mod. Phys.* **93**, 015004 (2021), [arXiv:2003.02206 \[hep-ph\]](#).
- [30] A. Berlin *et al.*, “Searches for New Particles, Dark Matter, and Gravitational Waves with SRF Cavities,” (2022), [arXiv:2203.12714 \[hep-ph\]](#).
- [31] T. Grenet, R. Ballou, Q. Basto, K. Martineau, P. Perrier, P. Pugnât, J. Quevillon, N. Roch, and C. Smith, “The Grenoble Axion Haloscope platform (GrAHal): development plan and first results,” (2021), [arXiv:2110.14406 \[hep-ex\]](#).
- [32] P. Pugnât, P. Camus, O. Kwon, R. Ballou, C. Bruyère, H. Byun, W. Chung, T. Grenet, P. Perrier, Y. K. Semertzidis, A. Talarmin, and J. Vessaire, *Front. Phys.* **12** (2024), [10.3389/fphy.2024.1358810](#).